A New Bimetallic Assembly Magnet $[\{Ni(tn)_2\}_5\{Fe^{III}(CN)_6\}_3]_n(ClO_4)_n\cdot 2.5nH_2O$ (tn = Trimethylenediamine) with a Novel 3-D Tunnel Structure

Si-Wei Zhang,[†] De-Gang Fu,[‡] Wei-Yin Sun,[†] Zheng Hu,[†] Kai-Bei Yu,[§] and Wen-Xia Tang*,[†]

Coordination Chemistry Institute and State Key Laboratory of Coordination Chemistry, Nanjing University, Nanjing 210093, China, National Laboratory of Molecular and Biomolecular Electronics, Southeast University, Nanjing 210096, China, and Analysis Center, Chengdu Branch of Chinese Academy of Science, Chengdu 610041, China

Received May 24, 1999

A novel molecular-based magnet of three-dimensional (3-D) cyanide-bridged bimetallic assembly, $[\{Ni(tn)_2\}_5\{Fe^{III}(CN)_6\}_3]_n(ClO_4)_n\cdot 2.5nH_2O$ where tn = trimethylenediamine, was synthesized and structurally characterized. The compound with an asymmetric unit of $C_{24}H_{52.5}Cl_{0.5}Fe_{1.5}N_{19}Ni_{2.5}O_{3.255}$ crystallized in the monoclinic system of the space group $P2_1/n$ with $a = 10.173(3)$ Å, $b = 16.053(2)$ Å, $c = 26.309(3)$ Å, $\beta = 91.30(2)°$, and $Z = 4$. The assembly has a 3-D network structure extended by three different types of $Fe^{III}-CN-Ni^{II}-NC-Fe^{III}$ linkages. The iron (Fe^{III}) atoms are located in two different chemical environments, which were confirmed by Mössbauer experimental results. The nickel (Ni^{II}) atoms have three different coordination environments. Cryomagnetic properties revealed that 3-D magnetic ordering occurs over the lattice below the Curie temperature around 10 K.

Introduction

The design and synthesis of well-characterized molecular-based magnets remains a challenge.[1−29] It is well-known that hexacyanometalate ions, $[M(CN)_6]^{3-}$, acting as good building blocks, play an important role in realizing bimetallic assemblies. Prussian blue and its analogues form a family of magnetic materials, and some assemblies with high Curie or Neel temperatures (T_C or T_N) have been reported.[18−28] However, magnetostructural correlation of these high-T_C or -T_N compounds remains unclear because of the difficulty of obtaining single crystals. Up to now, a series of bimetallic assemblies with two-dimensional (2-D) structures derived from a hexacyanometalate ion and a four-coordinate bis(diamine)−nickel(II) complex $[Ni(L)_2]^{2+}$ (L = diamine ligand) have been synthesized with the formula $[Ni(L)_2]_A[Fe(CN)_6]_BX\cdot nH_2O$ to explore the relationship between structure and magnetism.[7−10,30] Recently, several new bimetallic assemblies $[Ni^{II}(L)_2]_3[Fe^{II}(CN)_6]X_2$ (L = ethylenediamine, trimethylenediamine; $X = PF_6^-$, ClO_4^-) with a three-dimensional (3-D) network of the cubic Fe_8Ni_{12} unit using ferrocyanic anion $[Fe^{II}(CN)_6]^{4-}$ as a building block have been reported by Okawa and co-workers.[30] In our previous study, a bimetallic assembly of the $[\{(Cu(dien))_2Cr(CN)_6\}_n][Cu(dien)-$

* Corresponding author. Telephone: +86-25-3595706. Fax: +86-25-3314502. E-mail: wxtang@netra.nju.edu.cn.
[†] Nanjing University.
[‡] Southeast University.
[§] Chengdu Branch of Chinese Academy of Science.

(1) Kahn, O. *Advances in Inorganic Chemistry*; Academic Press, Inc.: San Diego, 1995; Vol. 43, p 179.
(2) Kahn, O. *Molecular Magnetism*; VCH: Weinheim, Germany, 1993.
(3) Miller, J. S.; Epstein, A. J. *Angew. Chem., Int. Ed. Engl.* **1994**, *33*, 385.
(4) Iwamura, H., Miller, A. S., Eds. Proceeding of the Conference on Chemistry & Physics of Molecular-Based Magnetic Materials. *Mol. Cryst. Liq. Cryst.* **1993**, 232−233.
(5) Gatteschi, D., Kahn, O., Miller, J. S., Palacio, F., Eds. *Molecular Magnetic Material*; NATO ASI Series E 198; Kluwer Academic Publishers: Dordrecht, 1990.
(6) Ohba, M.; Okawa, H. *Mol. Cryst. Liq. Cryst.* **1996**, *286*, 101.
(7) Ohba, M.; Maruono, N.; Okawa, H.; Enoki, T.; Latour, J. M. *J. Am. Chem. Soc.* **1994**, *116*, 11566.
(8) Ohba, M.; Okawa, H.; Ito, T.; Ohto, A. *J. Chem. Soc., Chem. Commun.* **1995**, 1545.
(9) Ohba, M.; Okawa, H.; Fukita, N.; Hashimoto, Y. *J. Am. Chem. Soc.* **1997**, *119*, 1011.
(10) Ohba, M.; Fukita, N.; Okawa, H. *J. Chem. Soc., Dalton Trans.* **1997**, 1733.
(11) Miyasaka, H.; Matsumoto, N.; Okawa, H.; Re, N.; Gallo, E.; Floriani, C. *Angew. Chem., Int. Ed. Engl.* **1995**, *34*, 1446.
(12) Miyasaka, H.; Matsumoto, N.; Okawa, H.; Re, N.; Gallo, E.; Floriani, C. *J. Am. Chem. Soc.* **1996**, *118*, 981.
(13) Re, N.; Gallo, E.; Floriani, C.; Miyasaka, H.; Matsumoto, N. *Inorg. Chem.* **1996**, *35*, 5964.
(14) Re, N.; Gallo, E.; Floriani, C.; Miyasaka, H.; Matsumoto, N. *Inorg. Chem.* **1996**, *35*, 6004.
(15) El Fallah, M. S.; Rentschler, E.; Caneschi, A.; Sessoli, R.; Gatteschi, D. *Angew. Chem., Int. Ed. Engl.* **1996**, *35*, 1947.
(16) Ferlay, S.; Mallah, T.; Vaissermann, J.; Bartolome, F.; Veillet, P.; Verdaguer, M. *Chem. Commun.* **1996**, 2481.
(17) Herren, F.; Fischer, P.; Ludi, A.; Hälg, W. *Inorg. Chem.* **1980**, *19*, 956.
(18) Klenze, R.; Kanellalopulos, B.; Trageser, G.; Eysel, H. H. *J. Chem. Phys.* **1980**, *72*, 5819.
(19) Griebler, W. D.; Babel, D. D. *Z. Naturforsch.* **1982**, *87B*, 832.
(20) Gadet, V.; Bujoli-Doeuff, M.; Force, L.; Verdaguer, M.; Malkhi, K. El; Deroy, A.; Besse, J. P.; Chappert, C.; Veillet, P.; Renard, J. P.; Beauvillain, P. In *Molecular Magnetic Material*; Gatteschi, D., et al., Eds.; NATO ASI Series 198; Kluwer: Dordrecht, 1990; p 281.
(21) Gadet, V.; Mallah, T.; Castro, I.; Verdaguer, M. *J. Am. Chem. Soc.* **1992**, *114*, 9213.
(22) Mallah, S.; Thiebaut, S.; Verdaguer, M.; Veillet, P. *Science* **1993**, *262*, 1554.
(23) Entley, W. R.; Girolani, G. S. *Science* **1995**, *268*, 397.
(24) Entley, W. R.; Girolani, G. S. *Inorg. Chem.* **1994**, *33*, 5165.
(25) Ferlay, S.; Mallah, T.; Ouahés, R.; Veillet, P.; Verdaguer, M. *Nature* **1995**, *378*, 701.
(26) Kahn, O. *Nature* **1995**, *378*, 667.
(27) Sato, O.; Iyoda, T.; Fujishima, A.; Hashimoto, K. *Science* **1996**, *271*, 49.
(28) Sato, O.; Iyoda, T.; Fujishima, A.; Hashimoto, K. *Science* **1996**, *271*, 704.
(29) Arrio, M. A.; Sainctavit, P.; Moulin, C. C.; Mallah, T.; Verdaguer, M.; Pellegrin, E.; Chen, C. T. *J. Am. Chem. Soc.* **1996**, *118*, 6422.
(30) (a) Fulita, N.; Ohba, M.; Okawa, H.; Matsuda, K.; Iwamura, H. *Inorg. Chem.* **1998**, *37*, 842. (b) Ohba, M.; Usuki, N.; Fukita, N.; Okawa, H. *Inorg. Chem.* **1998**, *37*, 3349.

10.1021/ic990591y CCC: $19.00
Published on Web 03/02/2000

$(H_2O)Cr(CN)_6]_n \cdot 4nH_2O$ (dien = diethylenetriamine) which has an infinite chainlike structure was obtained.[31,32] However, well-characterized 3-D bimetallic assemblies using ferricyanic anion $[Fe^{III}(CN)_6]^{3-}$ as a building block are very limited to our knowledge. Since the ferromagnetism itself is a three-dimensional property,[20] we devote our efforts to obtaining the 3-D bimetallic assemblies. Reported in this paper is a bimetallic assembly $[\{Ni(tn)_2\}_5\{Fe^{III}(CN)_6\}_3]_n(ClO_4)_n \cdot 2.5nH_2O$ (tn = trimethylenediamine) with a 3-D tunnel structure using hexacyanoferric anion, $[Fe^{III}(CN)_6]^{3-}$, as a building block. The crystal structure determined by X-ray crystallography indicates a 3-D network structure extended by three different types of $Fe^{III}-CN-Ni^{II}-NC-Fe^{III}$ linkages. Cryomagnetic properties revealed that three-dimensional magnetic ordering occurs over the lattice below the Curie temperature around 10 K.

Experimental Section

All chemicals and solvents used for synthesis are reagent grade.

$[\{Ni(tn)_2\}_5\{Fe^{III}(CN)_6\}_3]_n(ClO_4)_n \cdot 2.5nH_2O$. The tn ligand (0.17 mL, 2 mmol) was added to a 90 mL aqueous solution of $Ni(ClO_4)_2 \cdot 6H_2O$ (366 mg, 1 mmol) and formed a green solution, which was then added dropwise to a 150 mL aqueous solution of $K_3[Fe(CN)_6]$ (164.6 mg, 0.5 mmol) at room temperature. The resulting brown solution was allowed to stand for 1 week to form black red rhombic crystals. They were collected by suction filtration, washed with water, and dried in vacuo over P_2O_5. All the operations for the synthesis were carried out in the dark to avoid decomposition of the $K_3[Fe(CN)_6]$. Yield: 121 mg (34%). Anal. Calcd for $C_{48}H_{105}ClNi_5Fe_3N_{38}O_{6.5}$: C, 31.75; H, 5.83; N, 29.33; Fe, 9.23; Ni, 16.16. Found: C, 31.76; H, 6.23; N, 28.98; Fe, 8.86; Ni, 15.95.

Caution! *Perchlorate salts are potentially explosive and should be handled in small quantities.*

Physical Measurements. Mössbauer spectral measurements were carried out by using a constant acceleration Mössbauer spectrometer. All isomer shifts are relative to α-Fe. Magnetic susceptibilities were measured on a Quantum Design MPMS-5S SQUID susceptometer. Diamagnetic corrections were made using Pascal's constants for all the constituent atoms, and the magnetic moments were calculated using the equation $\mu = 2.828(\chi_M T)^{1/2}$. Field dependencies of magnetization were determined on the same susceptometer under an applied magnetic field up to 50 kG.

Structure Analysis. Single-crystal X-ray diffraction was measured on a Siemens P4 four-circle diffractometer with monochromated Mo Kα ($\lambda = 0.71073$ Å) radiation using the $\theta/2\theta$ scan mode with a variable scan speed 5.0−50.0 deg min^{-1} in ω. The relevant crystal data and structural parameters are summarized in Table 1.

The data were corrected with Lorentz and polarization effects during data reduction using XSCANS.[33] The structure was solved by a direct method and refined on F^2 by full-matrix least-squares methods using SHELXTL version 5.0.[34] All of the non-hydrogen atoms were refined anisotropically. All of the hydrogen atoms were placed in calculated positions (C−H, 0.96 Å; N−H, 0.90 Å) assigned fixed isotropic thermal parameters at 1.2 times the equivalent isotropic U of the atoms to which they are attached, and allowed to ride on their respective parent atoms. The contributions of these hydrogen atoms were included in the structure factor calculations.

The SHELXTL-Pc Program Package[34] was used for the computation. Analytical expressions of neutral-atom scattering factors were employed, and anomalous dispersion corrections were incorporated.[35]

Table 1. Crystallographic Data for $[\{Ni(tn)_2\}_5\{Fe(CN)_6\}_3]_n(ClO_4)_n \cdot 2.5nH_2O$

formula	$C_{24}H_{52.5}Cl_{0.5}Fe_{1.5}N_{19}Ni_{2.5}O_{3.255}$
fw	907.63
space group	$P2_1/n$
T/K	295(2)
λ/Å	0.71073
a/Å	10.173(3)
b/Å	16.053(2)
c/Å	26.309(3)
β/deg	91.30(2)
V/Å^3	4295.3(4)
Z	4
ρ_{calcd}/g cm^{-3}	1.404
μ/cm^{-1}	1.656
R1[a] [$I > 2\sigma(I)$]	0.0533
wR2[b] [$I > 2\sigma(I)$]	0.1260

[a] $R1 = \sum||F_o| - |F_c||/\sum|F_o|$, $wR2 = |\sum w(|F_o|^2 - |F_c|^2)|/\sum|w(F_o)^2|^{1/2}$. [b] $w = 1/[(F_o^2)^2 + (0.0691P)^2]$, where $P = (F_o^2 + 2F_c^2)/3$.

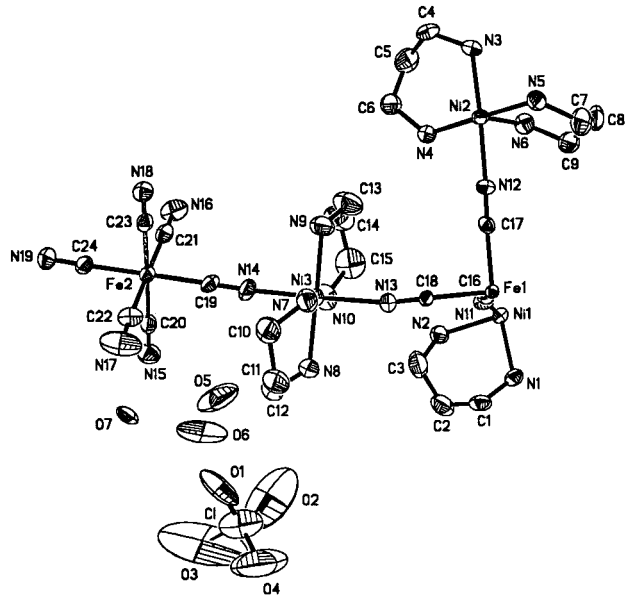

Figure 1. ORTEP representation of the asymmetric unit with atom-numbering scheme of the title assembly represented by 50% probability ellipsoids.

Results and Discussion

Crystal Structures. Figure 1 shows an ORTEP drawing of the asymmetric unit with an atom-numbering scheme of the assembly. The detailed coordination environment for all kinds of metal ions in the lattice is shown in Figure 2. Selected bond distances and angles with their estimated standard deviations are listed in Table 2. The asymmetric unit consists of a $^3/_2$ $[Fe(CN)_6]^{3-}$ (0.5 Fe1, 1.0 Fe2) anion and $^5/_2$ $[Ni(tn)_2]^{2+}$ (1.0 Ni2, 1.0 Ni3, and 0.5 Ni1) cation (see Figure 1). The metal ion of Fe1 is located at the special equivalent position (1, $^1/_2$, $^1/_2$), and each Fe1 ion connects to six nickel ions (Ni1, Ni1A, Ni2, Ni2A, Ni3, Ni3A) through six cyanide bridges. Each Fe2 ion links two nickel ions (Ni2A, Ni3) through two cyanide ions (C23N18, C19N14) in the cis position, and the other four cyano groups are nonbridging group (see Figure 2 and Supporting Information, Figure 1S). Thus, two kinds of iron atoms, Fe1 and Fe2, with different coordination environments exist in the crystal lattice of the title compound. All of the nickel atoms coordinate to six nitrogen atoms and have nearly octahedral

(31) Fu, D. G.; Chen, J.; Tan, X. S.; Jiang, L. J.; Zhang, S. W.; Zheng, P. J.; Tang, W. X. *Inorg. Chem.* **1997**, *36*, 220.
(32) Zhang, S. W.; Duan, C. Y.; Fu, D. G.; Tang, W. X.; Hu, C. H.; Chen, J.; Zheng, P. J. *Chem. J. Chin. Univ.* **1997**, *18*, 1019.
(33) *XSCANS (Version 2.1)*; Siemens Analytical X-ray Instruments Inc.: Madison, WI, 1994.
(34) *SHELXTL (Version 5.0)*; Siemens Industrial Automation, Inc, Analytical Instrumentation: Madison, WI, 1995.
(35) *International Tables for X-ray Crystallography*; Wilson, A. J. C., Ed.; Kluwer Academic Publishers: Dordrecht, 1992; Vol. C, Tables 6.1.1.4 (pp 500−502), 4.2.6.8 (pp 219−22), and 4.2.4.2 (pp 193−199).

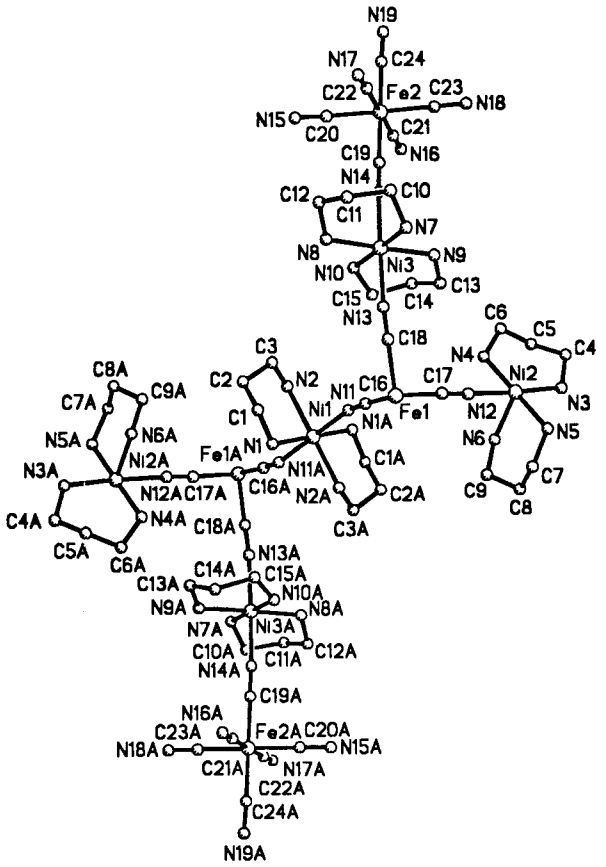

Figure 2. Coordination environment surrounding Fe1, Ni1, and Ni3 with the atom-numbering scheme.

geometry. The Ni1 atom resides at the special position ($^3/_2$, $^1/_2$, $^1/_2$) whose equatorial sites are occupied by the four nitrogen atoms (N1, N2, N1A, N2A) of two tn chelate ligands, while the two apical sites are occupied by the two cyano nitrogen atoms (N11, N11A). The bond linkage of Fe1−Ni1−Fe1A is in the trans position (see Figure 2). The Ni3 atom is not located at the special equivalent position. The coordination environment of Ni3 is similar to that for Ni1; four nitrogen atoms of tn ligand (N7, N8, N9, N10) occupied the equatorial position, while the two apical sites are occupied by the two cyano nitrogen atoms (N13, N14). The bond linkage of Fe1−Ni3−Fe2 is also in the trans form (see Figure 2). It is noticed that the coordination configuration of Ni2 is different from that of the above-mentioned nickel(II) (Ni1, Ni3) atoms. Although each Ni2 atom also coordinates to six nitrogen atoms and has a nearly octahedral geometry, the equatorial positions are occupied by three nitrogen atoms of two tn ligands (N3, N4, N5) and a cyano nitrogen atom (N12), and the other nitrogen atom of one tn ligand (N6) and a cyano nitrogen (N18A) occupied the apical sites. The bond linkage of Fe1−Ni2−Fe2A is in the cis form (see Figure 1S). Thus three different Ni atoms exist in the lattice due to the different configurations and occupy different sites in the crystal. The two kinds of linkage of Fe1−CN−Ni2−NC−Fe2B and Fe1−CN−Ni3−NC−Fe2 in the lattice spread along the *bc* plane to form 2-D sheets with 48-atom macrocyclic [$Fe1_4Fe2_4Ni2_4Ni3_4(CN)_{16}$] structures, and the third kind of Fe1−CN−Ni1−NC−Fe1A linkage is extended in a parallel direction with the *a* axis, which connects 2-D sheets to form a 3-D network structure as depicted in Figure 3. The perchlorate anions and water molecules are positioned in the tunnels. This novel 3-D network is different from the reported 3-D structure based on a cube formed by 8 $[Fe(CN)_6]^{4-}$ anions at the corners and 12 $[Ni(L)_2]^{2+}$ cations at the edges.[30] This is the first example of a 3-D bimetallic assembly with a tunnel structure, $[\{Ni(tn)_2\}_5\{Fe^{III}(CN)_6\}_3]_n(ClO_4)_n\cdot 2.5nH_2O$, in which the Fe atoms are in the oxidized state.

Table 2. Selected Bond Distances (Å) and Angles (deg) of $[\{Ni(tn)_2\}_5\{Fe(CN)_6\}_3]_n(ClO_4)_n\cdot 2.5nH_2O$[a]

Bond Distances (Å)			
Fe(1)−C(16)	1.939(7)	Ni(1)−N(11)	2.087(5)
Fe(1)−C(17)	1.964(7)	Ni(1)−N(1)	2.109(5)
Fe(1)−C(18)	1.949(6)	Ni(1)−N(2)	2.108(5)
Fe(2)−C(19)	1.929(7)	Ni(2)−N(12)	2.128(5)
Fe(2)−C(20)	1.944(8)	Ni(2)−N(18A)	2.094(6)
Fe(2)−C(21)	1.941(8)	Ni(2)−N(3)	2.120(5)
Fe(2)−C(22)	1.948(8)	Ni(2)−N(4)	2.096(5)
Fe(2)−C(23)	1.942(7)	Ni(2)−N(5)	2.100(5)
Fe(2)−C(24)	1.944(7)	Ni(2)−N(6)	2.128(5)
Ni(3)−N(13)	2.137(6)	Ni(3)−N(8)	2.103(5)
Ni(3)−N(14)	2.090(6)	Ni(3)−N(9)	2.091(6)
Ni(3)−N(7)	2.095(6)	Ni(3)−N(10)	2.099(6)

Bond Angles (deg)			
N(11)−Ni(1)−N(11A)	180.0	N(11)−Ni(1)−N(2A)	87.3(2)
N(11)−Ni(1)−N(1)	88.8(2)	N(2)−Ni(1)−N(1A)	91.1(2)
N(11)−Ni(1)−N(1A)	91.2(2)	N(2)−Ni(1)−N(1)	88.9(2)
N(11)−Ni(1)−N(2)	92.7(2)	N(6)−Ni(2)−N(4)	90.9(2)
N(18A)−Ni(2)−N(5)	89.9(2)	N(6)−Ni(2)−N(3)	91.4(2)
N(18A)−Ni(2)−N(3)	87.5(2)	N(4)−Ni(2)−N(5)	178.5(2)
N(18A)−Ni(2)−N(6)	178.9(2)	N(5)−Ni(2)−N(12)	91.2(2)
N(18A)−Ni(2)−N(4)	89.4(2)	N(12)−Ni(2)−N(4)	87.6(2)
N(18A)−Ni(2)−N(12)	89.8(2)	N(4)−Ni(2)−N(3)	91.2(2)
N(6)−Ni(2)−N(5)	89.9(2)	N(3)−Ni(2)−N(5)	90.1(2)
N(6)−Ni(2)−N(12)	91.2(2)	N(3)−Ni(2)−N(12)	177.1(2)
N(14)−Ni(3)−N(9)	88.5(3)	N(14)−Ni(3)−N(7)	92.1(3)
N(9)−Ni(3)−N(7)	91.0(3)	N(14)−Ni(3)−N(10)	88.3(3)
N(9)−Ni(3)−N(10)	91.2(3)	N(7)−Ni(3)−N(10)	177.7(3)
N(14)−Ni(3)−N(8)	90.9(2)	N(9)−Ni(3)−N(8)	177.2(3)
N(7)−Ni(3)−N(8)	86.2(2)	N(10)−Ni(3)−N(8)	91.5(3)
N(14)−Ni(3)−N(13)	177.7(2)	N(9)−Ni(3)−N(13)	89.5(2)
N(7)−Ni(3)−N(13)	89.0(2)	N(10)−Ni(3)−N(13)	90.6(3)
N(8)−Ni(3)−N(13)	91.2(2)	C(16)−Fe(1)−C(17)	88.6(3)
C(16)−Fe(1)−C(16A)	180.0	C(18A)−Fe(1)−C(17)	88.4(2)
C(16)−Fe(1)−C(18)	90.2(3)	C(16)−Fe(1)−C(17A)	91.4(3)
C(16)−Fe(1)−C(18A)	89.8(3)	C(18)−Fe(1)−C(17)	91.6(3)
C(19)−Fe(2)−C(21)	90.1(3)	C(19)−Fe(2)−C(23)	90.3(3)
C(21)−Fe(2)−C(23)	89.1(3)	C(19)−Fe(2)−C(20)	90.2(3)
C(21)−Fe(2)−C(20)	92.2(3)	C(23)−Fe(2)−C(20)	178.6(3)
C(19)−Fe(2)−C(24)	88.8(3)	C(21)−Fe(2)−C(24)	90.8(3)
C(23)−Fe(2)−C(24)	89.5(3)	C(20)−Fe(2)−C(24)	89.9(3)
C(19)−Fe(2)−C(22)	88.8(3)	C(21)−Fe(2)−C(22)	178.8(3)
C(23)−Fe(2)−C(22)	91.0(3)	C(20)−Fe(2)−C(22)	87.7(3)
C(24)−Fe(2)−C(22)	90.3(3)		

[a] Symmetry transformations used to generate equivalent atoms: A: $-x+3, -y+1, -z+2$.

Mössbauer Spectrum. The Mössbauer spectrum of the assembly recorded at room temperature is given in Figure 4, which shows an asymmetrical doublet indicating that there are two kinds of ferric (Fe^{III}) species in the crystal lattice. The corresponding Mössbauer parameters, obtained by the use of the least-squares methods, are IS(1) = −0.032 mm s^{-1}, QS(1) = 0.53 mm s^{-1} and IS(2) = 0.13 mm s^{-1}, QS(2) = 0.34 mm s^{-1}, which are considered to be originate from Fe1 and Fe2 atoms, respectively, in the crystal structure of the complex (Figure 1). The results indicate that the Fe(III) atoms in the complex are in the low-spin state.

Magnetic Properties. The cryomagnetic properties of a powder sample of $[\{Ni(tn)_2\}_5\{Fe^{III}(CN)_6\}_3]_n(ClO_4)_n\cdot 2.5nH_2O$ measured under 200 G are shown in Figure 5 in the form of the $\chi_M T$ vs T and χ_M^{-1} vs T plot. At room temperature, the $\chi_M T$ value is 3.66 cm^3 K mol^{-1} (5.41 μ_B per $Ni_{2.5}Fe_{1.5}$), which is slightly larger than the expected value for the noncoupled

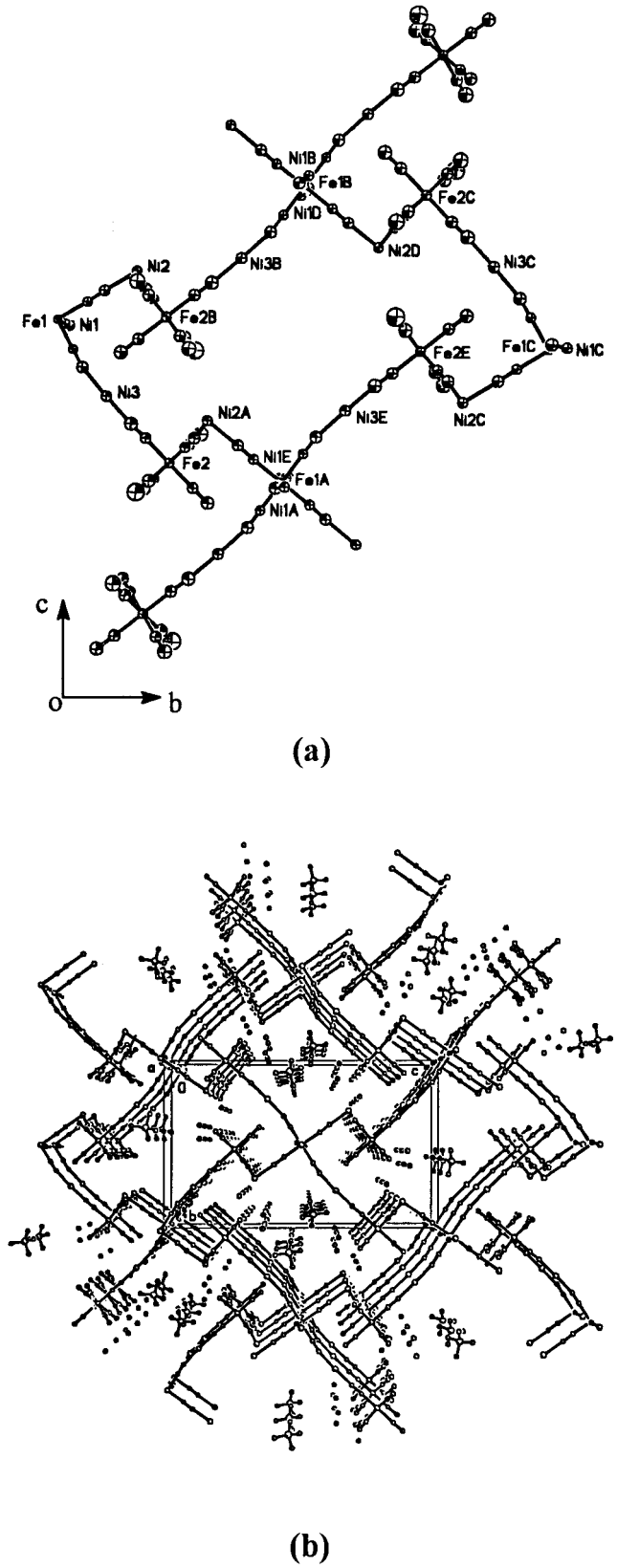

Figure 3. (a) View of the 48-atom macrocyclic $[Fe1_4Fe2_4Ni2_4Ni3_4(CN)_{16}]$ structure. Symmetry operator A: $0.5 - x, 0.5 + y, 0.5 - z$; B: $0.5 - x, -0.5 + y, 0.5 - z$. C, D, and E: $-x, -y, -z$. (tn ligands, perchlorate anions, and water molecules are omitted for clarity.) (b) View of 3-D network structure along the *a* axis for the title compound (tn ligands are omitted for clarity).

2.5 high-spin Ni(II) ($S = 1$) and 1.5 low-spin Fe(III) ions (3.06 cm^3 K mol^{-1}, 4.95 μ_B per $Ni_{2.5}Fe_{1.5}$, calculated using $g = 2.0$).

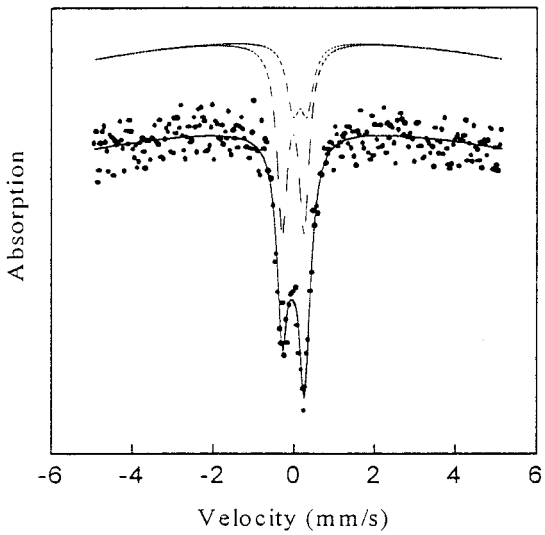

Figure 4. ^{57}Fe Mössbauer spectrum of $[\{Ni(tn)_2\}_5\{Fe(CN)_6\}_3]_n(ClO_4)_n \cdot 2.5nH_2O$ at room temperature.

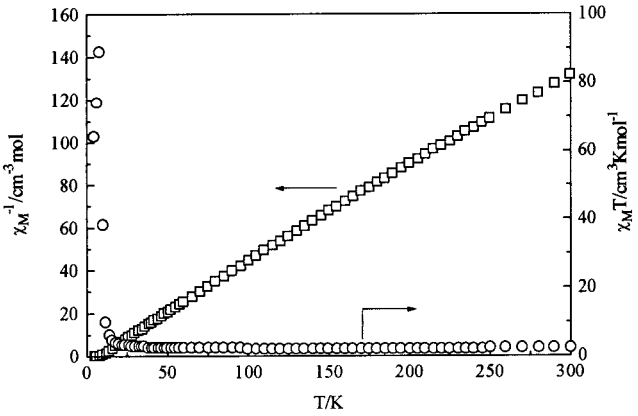

Figure 5. $\chi_M T$ vs T and χ_M^{-1} vs T plots of assembly per $Ni_{2.5}Fe_{1.5}$ unit ($\circ \rightarrow \chi_M T$ and $\square \rightarrow \chi_M^{-1}$).

The gradual decrease of the $\chi_M T$ value with temperature to the minimum value of 3.56 cm^3 K mol^{-1} (5.34 μ_B) at 150 K can be attributed to the orbital effect of the $^2T_2$ term of the low-spin Fe^{III} ion under O_h symmetry.[30] With further decreasing of the temperature, the value of $\chi_M T$ first increases gradually and then abruptly increases at about 10 K, reaching the value of 102.9 cm^3 K mol^{-1} (28.69 μ_B) at 5 K, which is significantly higher than that of the largest possible spin state $S_T = 6.5/2$, $\mu = 7.43$ μ_B (per $Ni_{2.5}Fe_{1.5}$). The sharp increase of the $\chi_M T$ at low temperature would suggest that the onset of a 3-D ferromagnetic ordering occurred. The χ_M^{-1} vs T plots in the range 5.001−150 K indicate the presence of a ferromagnetic exchange interaction between the low-spin Fe^{III} and Ni^{II} ions through the cyanide bridge. In accord with this, the Curie−Weiss plots in the temperature range 5−150 K gave a positive Weiss constant of $\Theta = +7.45$ K (based on $1/\chi_M = C(T - \Theta)$). The magnetic behavior below 150 K indicates a ferromagnetic interaction between the nearest Fe(III) and Ni(II) ions through the Fe^{III}−CN−Ni^{II} linkages. Ferromagnetic interaction between Fe(III) ($S = {}^1/_2$) and Ni(II) ($S = 1$) through the cyanide bridge is known and explained by the strict orthogonality of the magnetic orbital of the metal ions. The occurrence of a magnetic phase transition was established by measuring the magnetization as a function of magnetic field under a low temperature (5 K). The field-cooled magnetization (FCM) curve was obtained by cooling the sample from 100 to 5 K under a weak magnetic

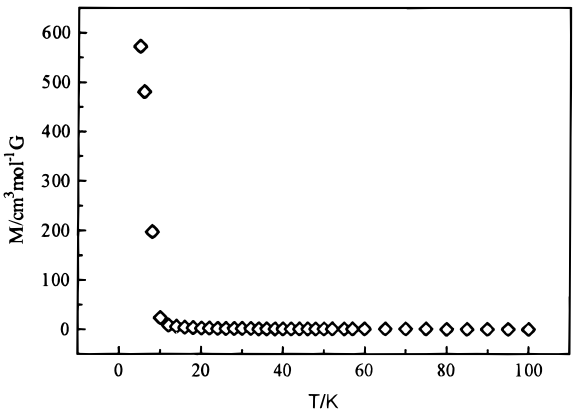

Figure 6. FCM (field-cooled magnetization vs *T*) curve under a weak magnetic field of 10 G per $Ni_{2.5}Fe_{1.5}$ unit.

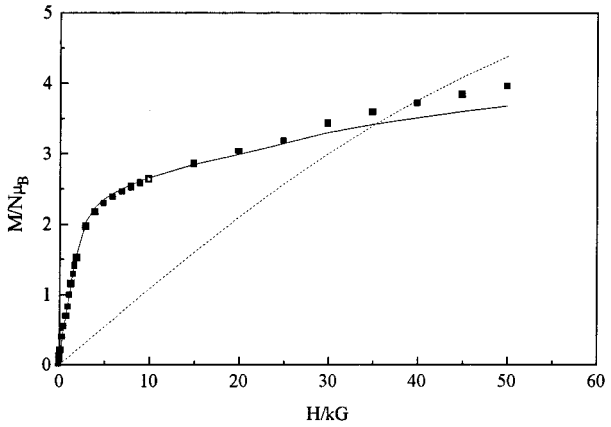

Figure 7. Field dependence of the magnetization at 5 K for the title compound per $Ni_{2.5}Fe_{1.5}$ unit. ■: experimental data. Solid line: the least-squares fitting of the experimental data with eq 1. Dashed curve: the calculated magnetization based on the Brillouin function for 2.5 isolated $S = 1$ Ni(II) ions and 1.5 $S = {}^1/_2$ Fe(III) ions.

field of 10 G and shows a rapid increase around 10 K (Figure 6). The ferromagnetic behavior of the title compound has been examined by the field dependence of magnetization measured at a temperature of 5 K (Figure 7). The magnetization curve per $Ni_{2.5}Fe_{1.5}$ shows a sharp increase from zero field. As seen from Figure 7, the magnetization per $Ni_{2.5}Fe_{1.5}$ at 50 kG is only 3.95 μ_B, far smaller than saturation value (6.5 μ_B). A similar case has been reported for $[Ni(tn)_2]_3[Fe(CN)_6](PF_6)_2$.[30a] The dashed curve in Figure 7 shows the calculated magnetization based on the Brillouin function for 2.5 isolated $S = 1$ Ni(II) ions and 1.5 $S = {}^1/_2$ Fe(III) ions. At weak magnetic field, the observed magnetization is larger than the calculated value, but above 40 kG, the calculated values are larger than the corresponding experimental values. These facts indicate the existence of canted spin magnetism in the title complex. The experimental magnetization at 5 K was treated by the mean-field model.[36,37]

The least-squares fitting of the experimental value with eq 1 gives $\Theta = 0.86$ K and $g = 2.01$ as shown by the solid line.

$$M = Ng\mu_B SB_s(\chi) \tag{1}$$

$$\chi = \frac{g\mu_B SH}{kT} + \frac{3\Theta}{g(S+1)TN\mu_B}M \tag{2}$$

It is seen that, at lower applied field, the experimental and theoretical values fitted very well, but at higher applied field, the theoretical value was smaller than the experimental value. This may be due to the spin cant as mentioned above. The fitting of experimental data measured under low applied field give similar values of $\Theta = 0.76$ K and $g = 2.04$ with much more goodness of fitting. The magnetic hysteresis loop of assembly (5 K) is shown in Figure 8. The remnant magnetization and the coercive field are 4226 cm^3 G mol^{-1} and 367 G, respectively. The above results clearly demonstrate the ferromagnetic nature of the title assembly.

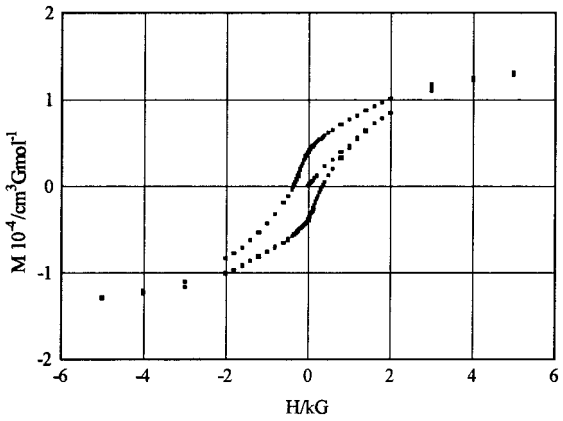

Figure 8. Magnetic hysteresis loop of assembly per $Ni_{2.5}Fe_{1.5}$ unit determined at 5 K.

Conclusion

This is the first example of a 3-D bimetallic assembly $[\{Ni(tn)_2\}_5\{Fe^{III}(CN)_6\}_3]_n(ClO_4)_n \cdot 2.5nH_2O$ with a tunnel structure in which Fe atoms are in the oxidized state. From the view of the structure, three points are very interesting: first, there are two different chemical environments of hexacyanoferric $[Fe(CN)_6]^{3-}$ in the crystal lattice; second, there is a 3-D network structure extended by three different $Fe^{III}-CN-Ni^{II}-NC-Fe^{III}$ linkages; third, tunnels exist in the crystal lattice along the *a* axis, and water molecules and perchlorate anions are located inside. Cryomagnetic property studies reveal that a three-dimensional magnetic ordering occurs over the crystal lattice, and the T_C of the assembly was determined to be around 10 K.

Acknowledgment. The National Natural Science Foundation of China and the Postdoctoral Science Foundation of China supported this work.

Supporting Information Available: Tables of crystallographic experimental data, all atoms introduced at calculated coordinates, anisotropic thermal parameters, and magnetic data (Tables S1−S6) and a figure showing the coordination environment of Ni2 and Fe2A atoms with atom-numbering scheme (Figure 1S) for the title complex. This material is available free of charge via the Internet at http://pubs.acs.org.

IC990591Y

(36) Veciana, J.; Rovica, C.; Ventosa, N.; Crespo, M. I.; Palacio, F. *J. Am. Chem. Soc.* **1993**, *115*, 57.
(37) Matsuda, K.; Nakamura, N.; Inoue, K.; Koga, N.; Iwamura, H. *Bull. Chem. Soc. Jpn.* **1996**, *69*, 1483.